Solid-State ^{17}O NMR Investigation of the Carbonyl Oxygen Electric-Field-Gradient Tensor and Chemical Shielding Tensor in Amides

Kazuhiko Yamada, Shuan Dong, and Gang Wu*

Contribution from the Department of Chemistry, Queen's University, Kingston, Ontario, Canada, K7L 3N6

Received March 7, 2000. Revised Manuscript Received July 11, 2000

Abstract: We have presented a systematic experimental and theoretical investigation of the carbonyl oxygen electric-field-gradient (EFG) tensor and chemical shielding (CS) tensor in crystalline amides. Three ^{17}O-labled secondary amides, $R_1C[^{17}O]\text{-}NHR_2$, have been synthesized: benzanilide (**1**), *N*-methylbenzamide (**2**), and acetanilide (**3**). Analysis of ^{17}O magic-angle spinning (MAS) and stationary NMR spectra yields not only the magnitude but also the orientation of the carbonyl ^{17}O EFG and CS tensors. For compounds **1**−**3**, the carbonyl ^{17}O quadrupolar coupling constant (QCC) and the span of the chemical shift tensor are found to be in the range of 8.5−8.97 MHz and 560−630 ppm, respectively. The largest ^{17}O EFG component lies in the amide plane and is perpendicular to the C═O bond, whereas the smallest component is perpendicular to the N−C═O plane. For the carbonyl ^{17}O CS tensor, the principal component with the largest shielding, δ_{33}, is perpendicular to the amide plane, and the tensor component corresponding to the least shielding, δ_{11}, is in the amide plane approximately 20° off the direction of the C═O bond. Extensive quantum chemical calculations using density functional theory (DFT) have been performed for both isolated and hydrogen-bonded molecules of compounds **1**−**3**. The calculated carbonyl ^{17}O EFG and CS tensors from the latter molecular models are in reasonably good agreement with the experimental values. In particular, the B3LYP/D95** EFG calculations overestimate the carbonyl ^{17}O QCC by approximately 0.5 MHz. The B3LYP/D95**/GIAO shielding calculations yield a linear correlation between the calculated and experimental data (slope = 1.125 and $R^2 = 0.9952$). The quantum chemical calculations indicated that the intermolecular C═O···H−N hydrogen-bonding interactions play an important role in determining the carbonyl oxygen EFG and CS tensors for an amide functional group.

Introduction

Together with hydrogen, carbon, and nitrogen, oxygen is among the most common elements in chemical substances. Although ^1H, ^{13}C, and ^{15}N nuclear magnetic resonance (NMR) spectroscopy has made a tremendous impact on the development of chemical and biological sciences, much less is known about ^{17}O NMR of organic and biological compounds. This is not surprising, because unfavorable nuclear properties of ^{17}O (spin = 5/2, natural abundance = 0.037%, $\gamma = -3.6279 \times 10^7$ rad T^{-1} s^{-1}, $Q \approx -2.558 \times 10^{-30}$ m^2) have rendered ^{17}O NMR experiments rather difficult. Nevertheless, solution ^{17}O NMR has been used for many years by organic chemists in the study of small molecules.[1−4] However, it is also clear that the rapid quadrupole relaxation property of ^{17}O has made solution ^{17}O NMR of biological macromolecules nearly impossible.

In principle, solid-state NMR spectra contain more information than the spectra obtained from liquids. More specifically, information regarding the orientation dependence of the fundamental NMR parameters (i.e., the tensorial property) is not directly available from solution NMR spectra. For ^{17}O NMR, the relevant NMR parameters are electric-field gradient (EFG) tensors and chemical shielding (CS) tensors. Recent advances in experimental solid-state NMR and computational chemistry have made it possible to establish a correlation between NMR tensors and molecular structures,[5,6] but to date, most successful solid-state NMR applications have focused only on spin-1/2 nuclei such as ^{13}C and ^{15}N.

High-resolution solid-state ^{17}O NMR was pioneered by Oldfield and co-workers.[7−9] These authors demonstrated that useful information can be extracted from central-transition magic-angle spinning (MAS) ^{17}O NMR spectra. However, the spectral resolution of MAS spectra is severely limited by incomplete averaging of the second-order quadrupole interactions. Later, the advent of dynamic-angle spinning (DAS) and double rotation (DOR) techniques made it possible to obtain solid-state ^{17}O NMR spectra with a site resolution similar to those in spin-1/2 spectra.[10−14] However, both DAS and DOR

* Corresponding author. Phone: 613-533-2644. Fax: 613-533-6669. E-mail: gangwu@chem.queensu.ca.

(1) Klemperer, W. G. *Angew. Chem., Int. Ed. Engl.* **1978**, *17*, 246.
(2) Kintzinger, J. P. In *NMR Basic Principles and Progress*; Diehl, P., Fluck, E., Kosfeld, R., Eds.; Springer-Verlag: Berlin, 1981; Vol. 17, pp 1−65.
(3) McFarlane, W.; McFarlane, H. C. E. In *Multinuclear NMR*; Mason, J., Ed.; Plenum Press: New York, 1987; Chapter 14, pp 403−416.
(4) *Oxygen-17 NMR Spectroscopy in Organic Chemistry*; Boykin, D. W., Ed.; CRC Press: Florida, 1991.
(5) *Nuclear Magnetic Shieldings and Molecular Structure*; Tossell, J. A., Ed.; Kluwer Academic Publishers: Dordrecht, The Netherlands, 1993.
(6) *Modeling NMR Chemical Shifts: Gaining Insight into Structure and Environment*; Facelli, J. C., de Dios, A. C., Eds.; ACS Symposium Series 732; Oxford University Press: Oxford, 1999.
(7) Schramm, S.; Kirkpatrick, R. J.; Oldfield, E. *J. Am. Chem. Soc.* **1983**, *105*, 2483.
(8) Schramm, S.; Oldfield, E. *J. Am. Chem. Soc.* **1984**, *106*, 2502.
(9) Walter, T. H.; Turner, G. L.; Oldfield, E. *J. Magn. Reson.* **1988**, *76*, 106.
(10) Chmelka, B. F.; Mueller, K. T.; Pines, A.; Stebbins, J.; Wu, Y.; Zwanziger, J. W. *Nature* **1989**, *339*, 42.

10.1021/ja0008315 CCC: $19.00
Published on Web 11/10/2000

experiments are technically demanding and have not found widespread applications in the study of organic and biological compounds. The recent invention of multiple-quantum magic-angle spinning (MQMAS) methodology[15,16] has provided experimentalists with a new tool for studying half-integer quadrupolar nuclei and, consequently, triggered a new wave of research interest in the field of quadrupolar NMR. Several groups have already reported ^{17}O MQMAS results.[17−20] Not surprisingly, all these ^{17}O MQMAS studies focused on inorganic systems in which the ^{17}O quadrupole interactions are reasonably small. Solid-state ^{17}O NMR studies of organic and biological compounds are still rare in the literature. Notable examples of solid-state ^{17}O NMR studies of biologically relevant systems are those by Oldfield and co-workers on various heme protein models.[21]

Among the numerous oxygen-containing functional groups, the secondary amide functional group, $R_1C(O)$-NHR_2, is of particular importance. This functional group constitutes the peptide bond of proteins. It is also present in nucleic acid bases such as thymine (T), uracil (U) and guanine (G). The C═O···H−N hydrogen bond (HB) plays a major role in determining the conformations of proteins and nucleic acids. Ando and co-workers[22] reported the first solid-state ^{17}O NMR investigation of peptides. They showed that ^{17}O NMR parameters are a sensitive probe to the hydrogen-bonding interactions. Unfortunately, the relatively low ^{17}O enrichment level in their polypeptide samples produced only low-quality ^{17}O NMR spectra, from which the authors reached an erroneous conclusion concerning the orientation of the ^{17}O CS tensor in the molecular frame. Recently, we determined unambiguously the absolute orientation of the carbonyl ^{17}O CS tensor for a primary amide, benzamide.[23] We also demonstrated the importance of including a complete network of intermolecular C═O···H−N interactions in the quantum chemical calculations of ^{17}O NMR tensors. In this contribution, we report a systematic solid-state ^{17}O NMR study of the carbonyl oxygen EFG and CS tensors for three ^{17}O-labled secondary amides: benzanilide (**1**), *N*-methylbenzamide (**2**) and acetanilide (**3**). We chose these secondary amides as models for the peptide bond in proteins because the carbonyl oxygen atom in each of the three amides is directly involved in a C═O···H−N hydrogen bond, a situation very similar to those found in polypeptides and proteins. Using relatively high levels of ^{17}O enrichment and a high-field instrument, we are able to obtain high quality solid-state ^{17}O NMR spectra and extract reliable information about ^{17}O NMR tensors in amides.

Scheme 1

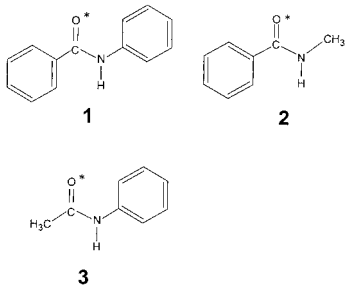

Theoretical background

In this section, we present the theoretical background for the analysis of ^{17}O NMR spectra arising from stationary powder samples. For a half-integer quadrupolar nucleus in a strong magnetic field, both the chemical shielding and second-order quadrupole interactions must be considered in order to calculate the central-transition (+1/2, −1/2) NMR spectra. The resultant NMR frequency can be written as a sum of three contributions:

$$\nu = \nu_0 + \nu_{CS} + \nu_Q^{(2)} \quad (1)$$

where ν_0 is the Larmor frequency, ν_{CS} and $\nu_Q^{(2)}$ are the chemical shielding and the second-order quadrupolar interaction contributions, respectively.

The nuclear quadrupolar interaction arises from the coupling between the nuclear quadrupole moment, Q, and the electric-field gradient (EFG) at the nuclear position. The EFG can be best described by a traceless second-rank tensor, whose principal components are defined as $|q_{zz}| > |q_{yy}| > |q_{xx}|$. In general, two other quantities are often used to describe a quadrupolar coupling tensor, namely, the quadrupole coupling constant (QCC), $\chi = e^2Qq_{zz}/h$, and the asymmetry parameter, $\eta = (q_{xx} - q_{yy})/q_{zz}$. For a half-integer quadrupolar nucleus ($I > 1/2$) in a strong magnetic field, only the second-order quadrupolar interaction needs to be considered for the central-transition (+1/2,−1/2) NMR spectra. The frequency contribution from the second-order quadrupolar interaction, $\nu_Q^{(2)}$, can be written as[24]

$$\nu_Q^{(2)} = (\nu_q^2/12\,\nu_0)\{3/2\,\sin^2\theta[(A+B)\cos^2\theta - B] - \eta\cos 2\phi\,\sin^2\theta[(A+B)\cos^2\theta + B] + (\eta/6)[A - (A+4B)\cos^2\theta - (A+B)\cos^2 2\phi(\cos^2\theta - 1)^2]\} \quad (2)$$

with

$$\nu_q = 3\chi/2I(2I-1) \quad (3)$$

$$A = 3 - 4I(I+1) \quad (4)$$

$$B = 1/4[3/2 - 2I(I+1)] \quad (5)$$

where θ and ϕ describe the orientation of the magnetic field in

(11) Wu, Y.; Sun, B. Q.; Pines, A.; Samoson, A.; Lippmaa, E. *J. Magn. Reson.* **1990**, *89*, 296.
(12) Mueller, K. T.; Sun, B. Q.; Chingas, Q. C.; Zwanziger, J. W.; Terao, T.; Pines, A. *J. Magn. Reson.* **1990**, *86*, 470.
(13) Mueller, K. T.; Wu, Y.; Chmelka, B. F.; Stebbins, J.; Pines, A. *J. Am. Chem. Soc.* **1991**, *113*, 32.
(14) Grandinetti, P. J.; Baltisberger, J. H.; Farnan, I.; Stebbins, J. F.; Werner, U.; Pines, A. *J. Phys. Chem.* **1995**, *99*, 12341.
(15) Frydman, L.; Harwood, J. S. *J. Am. Chem. Soc.* **1995**, *117*, 5367.
(16) Medek, A.; Harwood, J. S.; Frydman, L. *J. Am. Chem. Soc.* **1995**, *117*, 12779.
(17) Wu, G.; Rovnyak, D.; Sun, B. Q.; Griffin, R. G. *Chem. Phys. Lett.* **1996**, *249*, 210.
(18) Dirken, P. J.; Kohn, S. C.; Smith, M. E.; van Eck, E. R. H. *Chem. Phys. Lett.* **1997**, *266*, 568.
(19) Wu, G.; Rovnyak, D.; Huang, P. C.; Griffin, R. G. *Chem. Phys. Lett.* **1997**, *277*, 79.
(20) Stebbins, J. F.; Xu, Z. *Nature* **1997**, *390*, 60.
(21) (a) Salzmann, R.; Kaupp, M.; McMahon, M. T.; Oldfield, E. *J. Am. Chem. Soc.* **1998**, *120*, 4771. (b) McMahon, M. T.; de Dios, A. C.; Godbout, N.; Salzmann, R.; Laws, D. D.; Le, H.; Havlin, R. H.; Oldfield, E. *J. Am. Chem. Soc.* **1998**, *120*, 4784. (c) Godbout, N.; Sanders, L. K.; Salmann, R.; Havlin, R. H.; Wojdelski, M.; Oldfield, E. *J. Am. Chem. Soc.* **1999**, *121*, 3829.
(22) (a) Kuroki, S.; Takahashi, A.; Ando, I.; Shoji, A.; Ozaki, T. *J. Mol. Struct.* **1994**, *323*, 197. (b) Kuroki, S.; Ando, S.; Ando, I. *Chem. Phys.* **1995**, *195*, 107.
(23) Wu, G.; Yamada, K.; Dong, S.; Grondey, H. *J. Am. Chem. Soc.* **2000**, *122*, 4215.
(24) (a) Stauss, G. H. *J. Chem. Phys.* **1964**, *40*, 1988. (b) Amoureux, J.-P.; Fernandez, C.; Granger, P. In *Multinuclear Magnetic Resonance in Liquids and Solids-Chemical Applications*; Granger, P., Harris, R. K., Eds.; Kluwer Academic Publishes: Dordrecht, The Netherlands, 1990; pp 409−424. (c) Taulelle, F. In *Multinuclear Magnetic Resonance in Liquids and Solids-Chemical Applications*; Granger, P., Harris, R. K., Eds.; Kluwer Academic Publishes: Dordrecht, The Netherlands, 1990; pp 393−407.

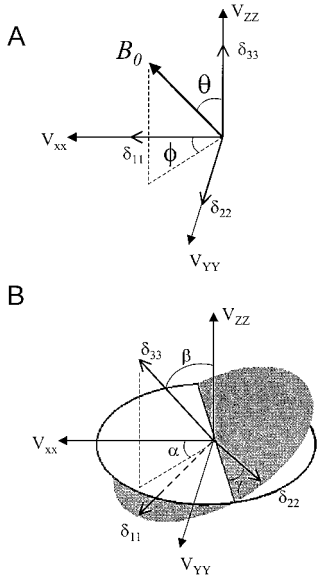

Figure 1. (A) Initial alignment of the ^{17}O EFG and CS tensors and direction of the external magnetic field, B_0. (B) Euler angles relating EFG and CS tensors.

the principal-axis system (PAS) of the EFG tensor as shown in Figure 1a.

For a chemical shielding (CS) tensor, we often use the following convention for the three principal components

$$\sigma_{11} \leq \sigma_{22} \leq \sigma_{33} \tag{6}$$

Therefore, the chemical shielding contribution to the NMR frequency is given by

$$\nu_{CS} = -\nu_0 (\sigma_{11}X^2 + \sigma_{22}Y^2 + \sigma_{33}Z^2) \tag{7}$$

where X, Y, and Z are the directional cosines of the external magnetic field in the PAS of the CS tensor. Note that the symbol σ is used for absolute chemical shielding and δ for chemical shift, $\delta_{11} \geq \delta_{22} \geq \delta_{33}$.

In general, the CS and EFG tensors have different orientations in the molecular frame of reference. Thus, we must consider the relative orientation between the two tensors using three Euler angles (α, β, γ). In this procedure, the new directional cosines (X', Y', Z') of the CS tensor with respect to the EFG system are used. Because the Euler angles describing the relative orientation of two tensors depend critically on the choice of initial frame and rotation sequence, confusion often arises in the literature as to which definition was actually used in the study. This sometimes makes it difficult to reproduce the reported tensor orientations. There are several different definitions in the literature concerning the Euler angles relating EFG and CS tensors and the initial alignment of the two tensors.[25] We believe that the approach of Eichele et al.[26] is the most straightforward procedure. Thus, we follow their procedure in the present study. The initial alignment of the two tensors is illustrated in Figure 1a. We can write the transformation matrix $A(\alpha, \beta, \gamma)$ as

$$A(\alpha, \beta, \gamma) = \begin{matrix} \cos\gamma\cos\beta\cos\alpha - \sin\gamma\sin\alpha & \cos\gamma\cos\beta\sin\alpha + \sin\gamma\cos\alpha & -\cos\gamma\sin\beta \\ -\sin\gamma\cos\beta\cos\alpha - \cos\gamma\sin\alpha & -\sin\gamma\cos\beta\sin\alpha + \cos\gamma\cos\alpha & \sin\gamma\sin\beta \\ \sin\beta\cos\alpha & \sin\beta\sin\alpha & \cos\beta \end{matrix} \tag{8}$$

Now the frequency contribution from the CS tensor can be expressed as

$$\nu_{CS} = -\nu_0(\sigma_{11}X'^2 + \sigma_{22}Y'^2 + \sigma_{33}Z'^2) \tag{9}$$

with

$$X' = \cos\gamma\cos\beta\, C + \sin\gamma\, D - \cos\gamma\sin\beta\cos\theta \tag{10}$$

$$Y' = \sin\gamma\cos\beta\, C + \cos\gamma\, D + \sin\gamma\sin\beta\cos\theta \tag{11}$$

$$Z' = \sin\beta\, C + \cos\beta\cos\theta \tag{12}$$

and

$$C = \sin\theta\cos\phi\cos\alpha + \sin\theta\sin\phi\sin\alpha \tag{13}$$

$$D = \sin\theta\sin\phi\cos\alpha - \sin\theta\cos\phi\sin\alpha \tag{14}$$

Combining Equations (1), (2), and (9), we can calculate ^{17}O NMR powder line shapes for stationary samples. Clearly, when (α, β, γ) = (0, 0, 0), the PAS of the CS tensor becomes coincident with that of the EFG tensor. Under such circumstances, all of the above equations are reduced to those reported by Baugher et al.[27]

Experimental and Computational Aspects

Sample Preparations. Benzoic acid-$^{17}O_2$ was prepared by reacting 0.3850 g (2.0 mmol) α,α,α-trichlorotoluene with 0.0720 g (4.0 mmol) H_2O* (50.8% ^{17}O atom purchased from ISOTEC, Miamisburg, Ohio) in a sealed tube at approximately 120 °C for 15 h. The resultant HCl gas was removed after cooling the sealed tube to room temperature. The remaining white crystalline products were recrystallized from acetone/petroether. Yield: 93%. [^{17}O]Benzoyl chloride was obtained by refluxing thionyl chloride and benzoic acid-$^{17}O_2$ (molar ratio of 1.1:1) for 1 h, and subsequently removing the excessive $SOCl_2$ by distillation. To [^{17}O]benzoyl chloride was added dropwise a cold phenylamine-methanol solution until the temperature was stabilized, and the solution was stirred at room temperature for 3 h. The solution was then poured into water, followed by extraction with diethyl ether. The white product of [^{17}O]benzanilide (**1**) (50.8% ^{17}O atom) was obtained upon removal of the solvent. [^{17}O]*N*-methylbenzamide (**2**) was synthesized by the same procedure as above except that a cold methylamine-methanol solution was used in the last step of the procedure. Acetic acid-$^{17}O_2$ was prepared by heating a mixture of 0.3 g (16.7 mmol) $H_2{}^{17}O$ and 0.35 g (8.5 mmol) acetonitrile in 8 mL anhydrous dioxane at 80 °C for 12 h. The solution was saturated with dry HCl gas before heating. Acetic acid-$^{17}O_2$ was converted to [^{17}O]-acetyl chloride by reaction with excessive $POCl_3$. [^{17}O]Acetyl chloride was separated by distillation. [^{17}O]Acetanilide (**3**) was obtained by reacting [^{17}O]acetyl chloride with excessive aniline in dioxane. Recrystallization yielded 140 mg of [^{17}O]acetanilide (total yield = 53%). The melting point, solution NMR, and IR results for compounds **1**−**3** are in agreement with the literature values.

Solid-State ^{17}O NMR. All ^{17}O NMR spectra were obtained on a Bruker Avance-500 NMR spectrometer operating at 500.13 and 67.8 MHz for ^1H and ^{17}O nuclei, respectively. Polycrystalline samples were packed into zirconium oxide rotors (4 mm o.d.). Typical sample

(25) (a) Cheng, J. T.; Edwards, J. C.; Ellis, P. D. *J. Phys. Chem*. **1990**, *94*, 553. (b) Power, W. P.; Wasylishen, R. E.; Mooibroek, S.; Pettitt, B. A.; Danchura, W. *J. Phys. Chem*. **1990**, *94*, 591. (c) Chu, P. J.; Gerstein, B. C. *J. Chem. Phys*. **1989**, *91*, 2081. (d) Man, P. P. In *Encyclopedia of Nuclear Magnetic Resonance*; Grant, D. M., Harris, R. K., Eds.; John Wiley & Sons: Chichester, U. K., 1996; Vol. 6, pp 3838−3848.

(26) (a) Eichele, K.; Chan, J. C. C.; Wasylishen, R. E.; Britten, J. F. *J. Phys. Chem. A* **1997**, *101*, 5423. (b) Eichele, K.; Wasylishen, R. E.; Nelson, J. H. *J. Phys. Chem. A* **1997**, *101*, 5463.

(27) Baugher, J. F.; Taylor, P. C.; Oja, T.; Bray, P. J. *J. Chem. Phys*. **1969**, *50*, 4914.

spinning frequencies were 12−15 kHz. For the stationary ^{17}O NMR experiments, a Hahn-echo sequence was used to eliminate acoustic ringing from the probe. Typical recycle delays were between 2 and 10 s. A liquid sample of H_2O (25% ^{17}O atom) was used for RF power calibration as well as for chemical shift referencing. Spectral simulations were performed with the WSOLIDS program package (Klaus Eichele and Rod Wasylishen, Dalhousie University).

Quantum Chemical Calculations. All quantum chemical calculations on ^{17}O EFG and CS tensors were carried out using the Gaussian98 program[28] on a Pentium II personal computer (400 MHz, 128 MB RAM, 12 GB disk space). The basis set of Dunning/Huzinaga double-ζ,[29] including polarization functions, D95**, and the B3LYP exchange functional[30] were employed. The Gauge-Included Atomic Orbital (GIAO) approach[31] was used for chemical shielding calculations. The experimental geometry of acetanilide determined by a neutron diffraction study[32] was used. For benzanilide and *N*-methylbenzamide, the crystal structures obtained from X-ray diffraction studies were used.[33,34] However, it is well-known that the N−H bond lengths measured by X-ray diffraction are generally not accurate as compared to those measured by the neutron diffraction technique. For this reason, the X-ray N−H bond lengths for benzanilide and *N*-methylbenzamide were corrected to a standard value, $r(\mathrm{N-H}) = 1.030$ Å.[35]

To make direct comparison between the calculated chemical shielding, σ, and the observed chemical shift, δ, we used the absolute ^{17}O chemical shielding scale established by Wasylishen and co-workers[36]

$$\delta = 307.9 \text{ ppm} - \sigma \qquad (15)$$

For the quadrupole interaction, because the quantum chemical calculations yield EFG tensor components, q_{ii}, in atomic units (a.u.), the following equation was used to convert them to the quadrupolar tensor components, χ_{ii}, in MHz

$$\chi_{ii}\,[\mathrm{MHz}] = e^2 Q q_{ii} h^{-1} = -2.3496 Q[\mathrm{fm}^2] q_{ii}\,[\mathrm{a.u.}] \qquad (16)$$

where Q is the nuclear quadrupole moment of the ^{17}O nucleus (in fm^2) and the factor of 2.3496 results from unit conversion. In the literature, the recommended Q value for ^{17}O is -2.558 fm^2.[37] However, several recent studies have demonstrated that, at different levels of theory, it is more advantageous to use "calibrated" Q values, rather than the standard Q value, to make direct comparison between the calculated and experimental ^{17}O QCCs.[38−40] Following this calibration approach, we obtained $Q(^{17}O) = -2.33$ fm^2 at the B3LYP/D95** level. This value is in excellent agreement with the calibrated Q value at similar DFT levels reported by De Luca et al.[40]

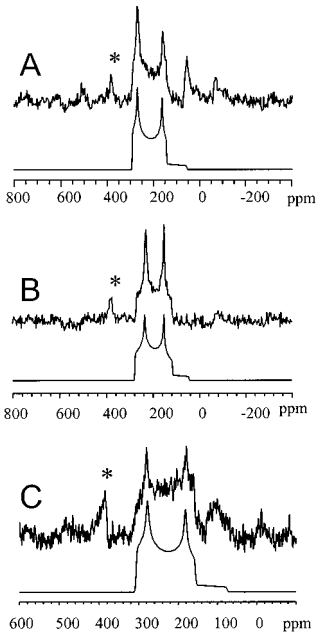

Figure 2. Experimental (upper trace) and calculated (lower trace) ^{17}O MAS NMR spectra for (A) [^{17}O]benzanilide (**1**), (B) [^{17}O]*N*-methylbenzamide (**2**), and (C) [^{17}O]acetanilide (**3**). The peaks marked by an asterisk (*) arise from the MAS rotor material, ZrO_2.

Results and Discussion

^{17}O EFG and CS Tensors. Figure 2 shows the experimental and simulated ^{17}O magic-angle spinning (MAS) NMR spectra for compounds **1**−**3**. Each of the MAS spectra exhibits a typical line shape arising from the second-order quadrupole interaction. The large line width of approximately 10−12 kHz indicates the presence of a sizable quadrupole coupling constant (QCC). From the spectral simulation, we were able to obtain the ^{17}O isotropic chemical shift, the QCC, and the asymmetry parameter for each of the three compounds. It should be noted that, because the spinning sideband intensities are not completely negligible, the simulated MAS line shapes shown in Figure 2 differ slightly from the experimental spectra at the low-frequency end of the line shape. The observed ^{17}O isotropic chemical shifts for compounds **1**−**3**, ca. 300 ppm, are typical for amide oxygen functional groups.[4] The magnitude of the carbonyl ^{17}O QCCs found for compounds **1**−**3**, ca. 8−9 MHz, is also consistent with previous determinations for the amide oxygen.[22,23,41] The detailed ^{17}O NMR results for compounds **1**−**3** are summarized in Table 1.

To obtain the information about the ^{17}O CS tensors, we obtained the stationary ^{17}O NMR spectra for compounds **1**−**3**. As shown in Figure 3, the stationary ^{17}O NMR spectra exhibit line shapes covering a frequency range of approximately 50 kHz, which is much larger than those of the MAS spectra. As already mentioned, analysis of the ^{17}O MAS spectra has yielded the isotropic ^{17}O chemical shift, QCC, and η. To analyze the stationary ^{17}O NMR spectra, we need to determine the remaining five variables: two independent CS tensor components and three

(28) Frisch, M. J.; Trucks, G. W.; Schlegel, H. B.; Scuseria, G. E.; Robb, M. A.; Cheeseman, J. R.; Zakrzewski, V. G.; Montgomery, J. A.; Stratmann, R. E.; Burant, J. C.; Dapprich, S.; Millam, J. M.; Daniels, A. D.; Kudin, K. N.; Strain, M. C.; Farkas, O.; Tomasi, J.; Barone, V.; Cossi, M.; Cammi, R.; Mennucci, B.; Pomelli, C.; Adamo, C.; Clifford, S.; Ochterski, J.; Petersson, G. A.; Ayala, P. Y.; Cui, Q.; Morokuma, K.; Malick, D. K.; Rabuck, A. D.; Raghavachari, K.; Foresman, J. B.; Cioslowski, J.; Ortiz, J. V.; Stefanov, B. B.; Liu, G.; Liashenko, A.; Piskorz, P.; Komaromi, I.; Gomperts, R.; Martin, R. L.; Fox, D. J.; Keith, T.; Al-Laham, M. A.; Peng, C. Y.; Nanayakkara, A.; Gonzalez, C.; Challacombe, M.; Gill, P. M. W.; Johnson, B.; Chen, W.; Wong, M. W.; Andres, J. L.; Head-Gordon, M.; Replogle, E. S.; Pople, J. A. Gaussian 98, Revision A.6; Gaussian, Inc.: Pittsburgh, PA, 1998.

(29) Dunning, T. H.; Hay, P. J. In *Modern Theoretical Chemistry*; Schaefer, H. F., Ed.; Plenum: New York, 1976; Vol. 3, p 1.

(30) (a) Becke, A. D. *Phys. Rev.* **1988**, *A38*, 3098. (b) Lee, C.; Yang, W.; Parr, R. G. *Phys. Rev.* **1988**, *B37*, 785. (c) Becke, A. D. *J. Chem. Phys*. **1993**, *98*, 5648.

(31) (a) Ditchfield, R. *Mol. Phys.* **1974**, *27*, 789. (b) Wolinski, K.; Hilton, J. F.; Pulay, P. *J. Am. Chem. Soc*. **1990**, *112*, 8257.

(32) Johnson, S. W.; Eckert, J.; Barthes, M.; McMullan, R. K.; Muller, M. *J. Phys. Chem*. **1995**, *99*, 16253.

(33) Kashio, S.; Ito, K.; Haisa, M. *Bull. Chem. Soc. Jpn*. **1979**, *52*, 365.

(34) Leiserowitz, L.; Tuval, M. *Acta Crystallogr*. **1978**, *B34*, 1230.

(35) (a) Taylor, R.; Kennard, O. *Acta Crystallgr*. **1983**, *B39*, 133. (b) Taylor, R.; Kennard, O.; Versichel, W. *Acta Crystallogr*. **1984**, *B40*, 280.

(36) Wasylishen, R. E.; Mooibroek, S.; Macdonald, J. B. *J. Chem. Phys*. **1984**, *81*, 1057.

(37) Pyykkö, P. *Z. Naturforsch*. **1992**, *47a*, 189.

(38) Eggenberger, R.; Gerber, S.; Huber, H.; Searles, D.; Welker, M. *J. Mol. Spectrosc*. **1992**, *151*, 474.

(39) (a) Ludwig, R.; Weinhold, F.; Farrar, T. C. *J. Chem. Phys.* **1995**, *103*, 6941. (b) Ludwig, R.; Weinhold, F.; Farrar, T. C. *J. Chem. Phys.* **1996**, *105*, 8223.

(40) De Luca, G.; Russo, N.; Köster, A. M.; Calaminici, P.; Jug, K. *Mol. Phys*. **1999**, *97*, 347.

(41) (a) Takahashi, A.; Kuroki, S.; Ando, I.; Ozaki, T.; Shoji, A. *J. Mol. Struct*. **1998**, *442*, 195. (b) Yamauchi, K.; Kuroki, S.; Ando, I.; Ozaki, T.; Shoji, A. *Chem. Phys. Lett*. **1999**, *302*, 331.

Table 1. Experimental ^{17}O CS and Quadrupole Coupling Tensors of the Carbonyl Oxygen in Compounds **1**−**3**[a]

system	δ_{iso}	δ_{11}	δ_{22}	δ_{33}	χ/MHz	η	deg α	deg β	deg γ
[^{17}O]benzanilide (**1**)	320	580	450	−50	8.97	0.15	5	90	70
[^{17}O]*N*-methylbenzamide (**2**)	287	520	380	−40	8.50	0.30	5	90	78
[^{17}O]acetanilide (**3**)	330	570	440	−20	8.81	0.20	0	89	69

[a] All chemical shifts are in ppm and relative to liquid water. Errors in the experimental CS principal components and χ are ± 5 ppm and ± 0.02 MHz, respectively. The uncertainty in the Euler angles is estimated to be ±4°.

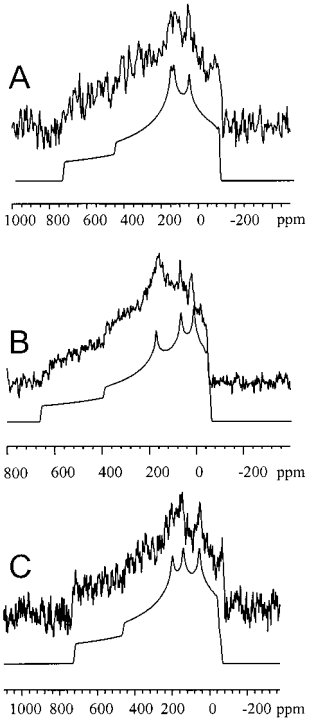

Figure 3. Experimental (upper trace) and calculated (lower trace) ^{17}O stationary NMR spectra for (A) [^{17}O]benzanilide (**1**), (B) [^{17}O]*N*-methylbenzamide (**2**), and (C) [^{17}O]acetanilide (**3**).

Euler angles that define the relative orientation between the EFG and CS tensors. In general, it is quite difficult or impossible to determine five unknowns from analyzing stationary ^{17}O NMR spectra obtained at a single field strength. The ideal technique for obtaining complete formation about NMR tensors is the single-crystal NMR experiment. However, large single crystals suitable for NMR experiments are often difficult to obtain. In the case of ^{17}O NMR, the necessity of introducing ^{17}O-lables makes it even more difficult to grow large single crystals because of the small quantity of labeled samples. Recently, we have combined multiple-field ^{17}O NMR experiments with quantum chemical calculations and established the absolute orientation of the ^{17}O EFG and CS tensors for the carbonyl oxygen in benzamide.[23] Using the result for benzamide as a starting point, we were able to analyze the experimental ^{17}O NMR spectra shown in Figure 3 in a straightforward fashion. The magnitude and orientation of the carbonyl ^{17}O EFG and CS tensors for compounds **1**−**3** are presented in Table 1 and illustrated in Figure 4. The spans of the carbonyl ^{17}O chemical shift tensors for compounds **1**−**3** are larger than that in benzamide, 500 ppm. The larger spans in **1**−**3** result mainly from opposite changes in δ_{11} and δ_{33}. In particular, for compound **1** (benzanilide), $\delta_{11} = 570$ ppm, and $\delta_{33} = -50$ ppm, whereas for benzamide, $\delta_{11} = 500$ ppm, and $\delta_{33} = 0$ ppm.

As also seen from Table 1, the ^{17}O CS tensors of compounds **1**−**3** show very similar orientations with respect to the corresponding EFG tensors, that is, $\alpha \approx 0°$, $\beta \approx 90°$, and $\gamma \approx 70°$.

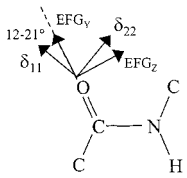

Figure 4. Orientations of ^{17}O EFG and CS tensors in the molecular frame. Both δ_{33} and EFG$_X$ components are perpendicular to the amide plane.

As depicted in Figure 4, the principal CS tensor component with the strongest shielding, δ_{33}, is approximately perpendicular to the N−C═O plane. The tensor component corresponding to the least shielding, δ_{11}, lies in the N−C═O plane approximately 20° off the C═O bond direction. This observation is consistent with the previous determination for benzamide.[23] The q_{xx} of the ^{17}O EFG tensor lies perpendicular to the amide plane. The q_{zz} component lies in the N−C═O plane and is perpendicular to the C═O bond. The experimental orientations of the ^{17}O EFG and CS tensors for compounds **1**−**3** are also in excellent agreement with the results of several previous quantum chemical calculations.[42−44] As will be discussed in the next section, the ^{17}O CS and EFG tensor orientations shown in Figure 4 are confirmed by quantum chemical calculations.

Quantum Chemical Calculations. Another objective of the present work is to evaluate the quality of quantum chemical calculations for ^{17}O EFG and CS tensors in hydrogen-bonded systems. Although there has been a considerable amount of theoretical work on ^{17}O chemical shielding constants in small molecules,[45−53] relatively little data are available concerning ^{17}O chemical shift tensors, especially for hydrogen-bonded molecular systems. We have recently shown that, to reproduce the experimental ^{17}O NMR results for an amide oxygen, it is necessary to include a complete intermolecular HB network in the quantum chemical calculations.[23] The carbonyl oxygen in each of the secondary amide systems studied here is directly

(42) Palmer, M. H. *Z. Naturforsch*. **1996**, *51A*, 442.
(43) Sitkoff, D.; Case, D. A. *Prog. Nucl. Magn. Reson. Spectrosc*. **1998**, *32*, 165.
(44) (a) Chesnut, D. B.; Phung, C. G. In *Nuclear Magnetic Shieldings and Molecular Structure*; Tossell, J. A., Ed.; Kluwer Academic Publishers: Dordrecht, The Netherlands, 1993; p 221. (b) Chesnut, D. B. *Annu. Rep. NMR Spectrosc*. **1994**, *29*, 71.
(45) Kutzelnigg, W.; Fleischer, U.; Schindler, M. In *NMR − Basic Principles and Progress*; Springer-Verlag: Berlin, 1990; Vol. 23, p 165.
(46) Chesnut, D. B.; Phung, C. G. *J. Chem. Phys*. **1989**, *91*, 6238.
(47) Kaupp, M.; Malkin, V. G.; Malkina, O. L.; Salahub, D. R. *J. Am. Chem. Soc*. **1995**, *117*, 1851.
(48) (a) Schreckenbach, G.; Ziegler, T. *J. Phys. Chem*. **1995**, *99*, 606. (b) Ruiz-Morales, Y.; Schreckenbach, G.; Ziegler, T. *J. Phys. Chem*. **1996**, *100*, 3359.
(49) (a) Gauss, J. *Chem. Phys. Lett*. **1992**, *191*, 614. (b) Gauss, J.; Stanton, J. F. *J. Chem. Phys*. **1996**, *104*, 2574.
(50) Hansen, P. E.; Abildgaard, J.; Hansen, A. E. *Chem. Phys. Lett*. **1994**, *224*, 275.
(51) Barszczewicz, A.; Jaszunski, M.; Jackowski, K. *Chem. Phys. Lett*. **1993**, *203*, 404.
(52) Olah, G. A.; Burrichter, A.; Rasul, G.; Gnann, R.; Christe, K. O.; Prakash, G. K. S. *J. Am. Chem. Soc*. **1997**, *119*, 8035.
(53) Kaupp, M.; Malkina, O. L.; Malkin, V. G. *J. Chem. Phys*. **1997**, *106*, 9201.

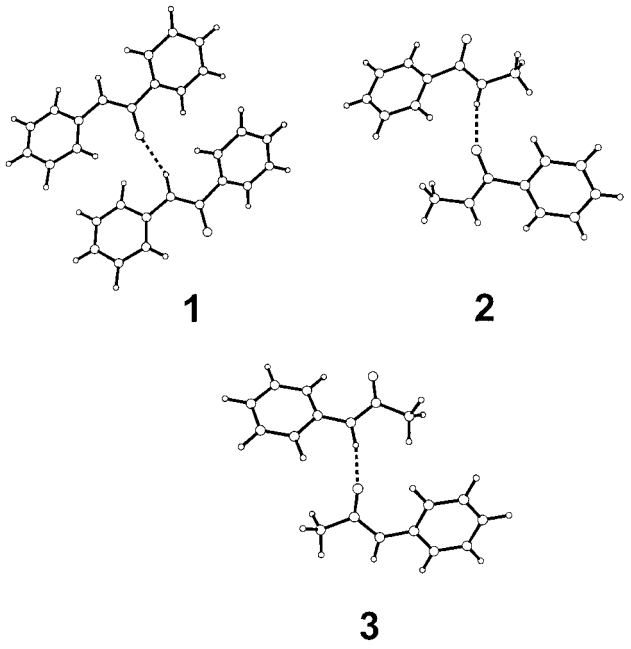

Figure 5. Hydrogen-bonded dimers used in the quantum chemical calculations of compounds **1** (A), **2** (B), and **3** (C).

involved in a single C═O···H−N hydrogen bond and, therefore, represents a good model for testing the performance of quantum chemical calculations in handling weak hydrogen bonds. The crystals of compound **1** are monoclinic in space group $C2/c$.[33] The molecules are linked together by a C═O···H−N hydrogen bond to form a chain along the *b* axis. The O···N distance is 3.112 Å. Compound **2** crystallizes in space group *Pbca*.[34] The hydrogen-bonded molecules are related to each other by a 2_1 axis with an O···N hydrogen-bond distance of 2.93 Å. Compound **3** is isostructural with compound **2** with similar unit cell dimensions, for which the O···N hydrogen-bond distance is 2.935 Å.[32]

To demonstrate the importance of including intermolecular HB interactions, we performed two sets of calculations. First, we calculated the ^{17}O EFG and CS tensors for isolated molecules (monomers) of compounds **1**−**3**. In the second set of calculations, we included a neighboring molecule that serves as the hydrogen-bond donor. The hydrogen-bonded molecular dimers used in the quantum chemical calculations for compounds **1**−**3** are shown in Figure 5. The calculated carbonyl ^{17}O CS and EFG tensors are presented in Table 2. Figure 6 shows the comparison between the experimental and calculated ^{17}O CS tensors for compounds **1**−**3**. Clearly, the calculated ^{17}O CS tensor components for monomers deviate significantly from the observed values. The largest deviations occur at δ_{11} components, ca. 160 ppm. For the hydrogen-bonded dimers, the calculations show a remarkable improvement. For example, the deviations between the calculated and observed δ_{11} components are reduced by 50%, ca. 80 ppm. As seen from Figure 6, the data from the dimer models produce a slope of 1.125, which compares to 1.261 from the calculations for monomers. Interestingly, the two models predict nearly identical orientations for the carbonyl ^{17}O CS tensor. This seems to suggest that only the magnitude of the individual components of the carbonyl ^{17}O CS tensor is sensitive to HB interactions. It should be emphasized that, because the present amide systems exhibit relatively weak HB interactions, it would be dangerous to generalize this observation. More studies are clearly required to reach a general understanding about the effects of intermolecular HB interactions on the orientation of the ^{17}O CS tensor.

Similar to the ^{17}O chemical shielding calculations, the dimer models also produce improved ^{17}O EFG results for compound **1**−**3**. As shown in Table 2, inclusion of the hydrogen-bonding interaction causes a reduction in the calculated ^{17}O QCCs. This is consistent with the general observation that hydrogen-bonding interactions tend to reduce the QCC at the ^{17}O nucleus.[23,54−56] At the B3LYP/D95** level of theory, the calculated ^{17}O QCCs are uniformly smaller than the corresponding experimental values by approximately 0.5 MHz. Again, the orientation of the carbonyl ^{17}O EFG tensor showed very little variation between the monomer and dimer models, despite the clear sensitivity of the magnitude of individual components to the models (vide infra).

The Hydrogen-Bonding Effects. In the preceding section, we demonstrated that the hydrogen-bonding interactions in compounds **1**−**3** are important. Because C═O···H−N hydrogen bonds are ubiquitous in biological systems, it is, therefore, of interest to examine the hydrogen-bonding effects on ^{17}O NMR tensors in more details. In this section, we construct a simple model containing an *N*-methylacetamide molecule and a formamide molecule (see Figure 7). The two molecules are individually optimized in their geometry and are placed together so that the two amide planes are coincident. Furthermore, the O···H−N hydrogen bond is assumed to be linear with the C═O···H angle being 120°. Such a model was used previously by de Dios and Oldfield in the study of the ^{13}C CS tensor as a function of HB geometry.[57] The major conclusion of their study is that the C═O bond length change upon hydrogen-bonding plays a major role in determining the ^{13}C CS tensor for the carbonyl carbon. Because the carbonyl oxygen atom is directly involved in the hydrogen-bonding, it is expected that both the lengthening of the C═O bond and the presence of the hydrogen-bond donor would be important to the ^{17}O NMR tensors. Our recent quantum chemical calculations on the ^{17}O NMR tensor of an oxonium ion revealed that the presence of the hydrogen-bond partner is, in fact, more important than the actual structural change of the H_3O^+ ion itself.[56] For these reasons, we decided to investigate the dependence of the carbonyl ^{17}O NMR tensors on the C═O bond length and on the O···N hydrogen-bond distance separately. In the present work, we report the results for the hydrogen-bond distance dependence. In the calculations, the hydrogen-bond distance, r(O···N), was varied (2.500, 2.800, 3.200, and 3.500 Å) and the hydrogen-bond angle (∠C═O···N) and the C═O bond length were kept constant at 120° and 1.230 Å, respectively. Our calculated results for the carbonyl ^{13}C CS tensor (data not shown) are in agreement with those reported by de Dios and Oldfield,[57] thus confirming the validity of our model. Table 3 summarizes the results of the ^{17}O EFG and CS tensor calculations for the *N*-methylacetamide/formamide model.

Figure 8 displays the dependence of both the ^{17}O CS tensor components and the isotropic chemical shift on the hydrogen-bond distance, r(O···N). All three tensor components changed linearly with r(O···N). Although δ_{11} and δ_{22} increased with r(O···N), δ_{33} exhibited an opposite trend. As a result, the isotropic chemical shift increased linearly with the hydrogen-bond distance. This is in qualitative agreement with previous findings from solution ^{17}O NMR studies that the stronger the HB interaction, the more shielded the carbonyl oxygen environ-

(54) (a) Butler, L. G.; Cheng, C. P.; Brown, T. L. *J. Am. Chem. Soc.* **1981**, *103*, 2738. (b) Butler, L. G.; Brown, T. L. *J. Am. Chem. Soc.* **1981**, *103*, 6541.
(55) Gready, J. E. *J. Phys. Chem.* **1984**, *88*, 3497.
(56) Wu, G.; Hook, A.; Dong, S.; Yamada, K. *J. Phys. Chem. A* **2000**, *104*, 4102.
(57) de Dios, A. C.; Oldfield, E. *J. Am. Chem. Soc.* **1994**, *116*, 11485.

Table 2. Calculated (B3LYP/D95**) Carbonyl ^{17}O CS and Quadrupole Coupling Tensors for Compounds **1**−**3**[a]

system	model	δ_{iso}	δ_{11}	δ_{22}	δ_{33}	χ_{zz}	χ_{yy}	χ_{xx}	deg α	deg β	deg γ
benzanilide (**1**)	monomer	403	740	508	−39	9.661	−6.634	−3.087	−2.4	89.3	78.1
	dimer	372	667	477	−27	9.366	−6.799	−2.567	2.0	90.4	76.6
N-methylbenzamide (**2**)	monomer	356	673	467	−71	9.147	−5.611	−3.536	2.0	89.9	85.4
	dimer	326	598	434	−55	8.769	−5.611	−3.536	−0.7	89.9	84.0
acetanilide (**3**)	monomer	394	732	499	−50	9.399	−5.529	−3.870	5.4	90.4	75.6
	dimer	363	659	464	−33	9.005	−5.808	−3.197	5.9	90.5	74.4

[a] All CS tensor components are in parts per million (ppm) and quadrupole coupling tensor components are in MHz.

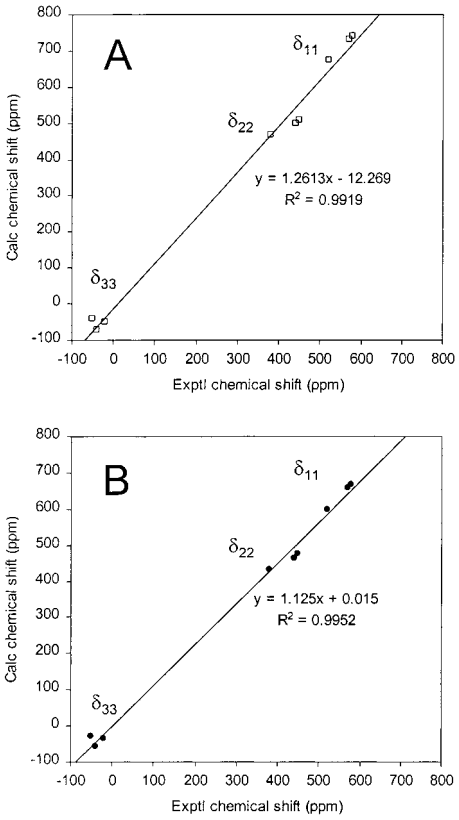

Figure 6. Comparison between experimental and calculated ^{17}O CS tensors for (A) monomers and (B) dimers.

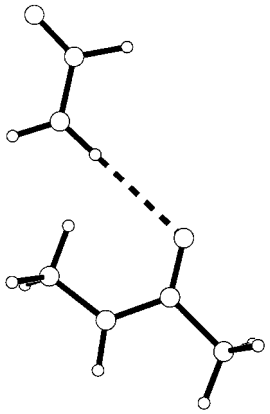

Figure 7. Model consisting of *N*-methylacetamide and formamide molecules linked by a C═O···H−N hydrogen bond.

ment is. In a previous theoretical work, Kuroki et al. investigated the HB effect on ^{17}O NMR tensors in a model containing *N*-acetyl-*N*′-methylglycine and two formamide molecules.[22b] They showed that all three CS tensor elements increased with the HB length. Our results are in general agreement with those of Kuroki et al. except for the opposite trend found for δ_{33}.

Table 3. Calculated (B3LYP/D95**) Carbonyl ^{17}O CS and Quadrupole Coupling Tensors for the *N*-methylacetamide/Formamide Complex[a]

O···N distance (Å)	δ_{iso}	δ_{11}	δ_{22}	δ_{33}	χ_{zz}	χ_{yy}	χ_{xx}
2.500	336	589	416	2	1.487	−1.068	−0.419
2.800	340	607	435	−21	1.491	−1.028	−0.463
3.200	345	627	451	−43	1.512	−1.002	−0.509
3.500	348	639	459	−53	1.530	−0.994	−0.536

[a] All CS tensor components are in parts per million (ppm) and quadrupole tensor components are in MHz.

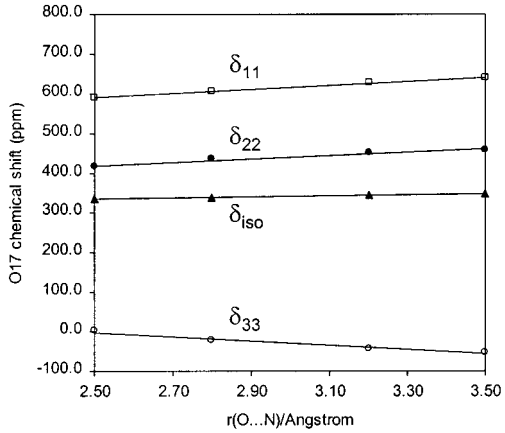

Figure 8. Calculated ^{17}O CS tensor components versus *r*(O···N) for the *N*-methylacetamide/formamide model.

The discrepancy may be due to the semiempirical method and a small basis set STO-6G used in the study of Kuroki et al. It is also seen from Figure 8 that tensor components are approximately four times more sensitive to the hydrogen-bond distance than is the isotropic chemical shift.

Figure 9 shows the dependence of the carbonyl ^{17}O QCC and asymmetry parameter on *r*(O···N). Clearly, the carbonyl ^{17}O QCC increases with *r*(O···N). This is consistent with the experimental observations for compounds **1**−**3**. For example, compound **1** exhibits the weakest hydrogen-bond strength, with *r*(O···N) = 3.112 Å, and the largest ^{17}O QCC, χ = 8.97 MHz. It is also interesting to note that because two C═O···H−N hydrogen bonds are present in benzamide (*r*(O···N) = 2.898 and 2.932 Å[58]) the carbonyl ^{17}O QCC is rather small, χ = 8.40 MHz.[23] Figure 9a suggests that for the model used in this study, the dependence of carbonyl ^{17}O QCC on *r*(O···N) is not linear. In fact, there is no theoretical reason for this dependence to be linear. Therefore, the previous observation of a linear relationship between ^{17}O QCC and *r*(O···N) may be either accidental or due to the small range of ^{17}O QCC values.[22a]

Another interesting finding is that the asymmetry parameter also exhibits a correlation with the hydrogen-bond distance. As

(58) Gao, Q.; Jeffrey, G. A.; Ruble, J. R. *Acta Crystallgr.* **1991**, *B47*, 742.

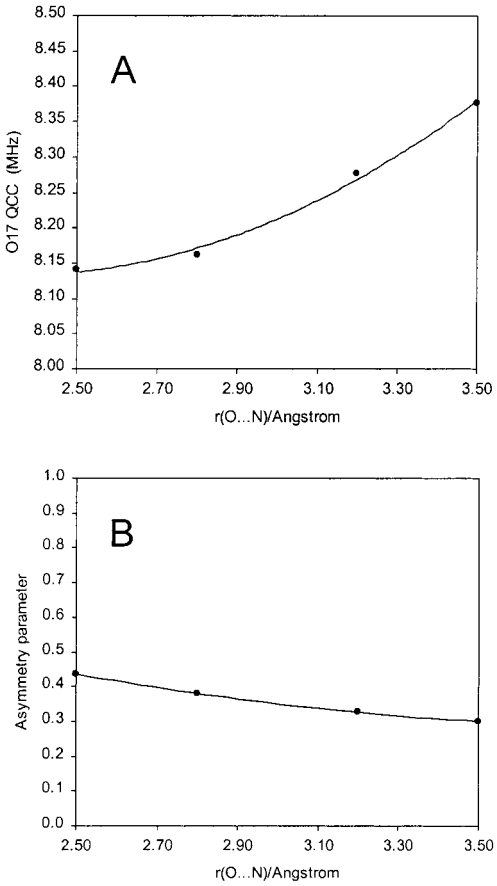

Figure 9. Calculated ^{17}O QCC (A) and asymmetry parameter (B) versus r(O···N) for the *N*-methylacetamide/formamide model.

seen from Figure 9b, the asymmetry parameter decreases with the hydrogen-bond length. This prediction is confirmed by the experimental data for compounds **1**−**3**. Specifically, compound **1**, which has a relatively long r(O···N), exhibits a carbonyl ^{17}O EFG tensor with $\eta = 0.15$. The asymmetry parameters from compounds **2** and **3** are 0.30 and 0.20, respectively. We also noticed that the asymmetry parameter for the ^{17}O EFG tensor of benzamide is even larger, $\eta = 0.37$.[23] From the data shown in Table 3, it is clear that the observed dependence for η arises from the fact that as r(O···N) is changed, q_{zz} and q_{xx} change in opposite directions, whereas q_{yy} remains approximately constant. This interesting observation in amides is consistent with the early ^{17}O NQR results reported by Cheng and Brown.[59]

Conclusions

We have presented a systematic investigation of ^{17}O CS and EFG tensors for secondary amide functional groups. The experimental and theoretical results have indicated that both ^{17}O CS and EFG tensors of an amide functional group are sensitive to the C═O···H−N hydrogen-bonding environment. In particular, δ_{11} and δ_{22} components increase with hydrogen-bond distance, whereas δ_{33} exhibits an opposite dependence. For the carbonyl ^{17}O quadrupolar coupling tensor, both ^{17}O QCC and the asymmetry parameter depend on the hydrogen-bond distance. We have also shown that it is important to obtain high-quality solid-state ^{17}O NMR spectra in order to extract reliable information about ^{17}O NMR tensors. At the B3LYP/D95** level, the quantum chemical calculations have reproduced the experimental ^{17}O QCC values within 0.5 MHz, whereas the correlation between the calculated and experimental ^{17}O CS tensor components exhibits a slope of 1.125 ($R^2 = 0.9952$). The benchmark experimental values reported in this study may be useful in testing future quantum chemical calculations for C═O···H−N hydrogen-bonded systems. The implication of the present study is that solid-state ^{17}O NMR is potentially useful as an additional nuclear probe in the study of proteins.

Acknowledgment. This research was supported by the Natural Sciences and Engineering Research Council (NSERC) of Canada. We wish to thank Dr. Klaus Eichele for providing the WSOLIDS program and for stimulating discussions. We are also grateful to Dr. Minhhuy Ho, Dr. Mike Lumsden, and Prof. Rod Wasylishen for helpful discussions and to an anonymous reviewer for very helpful comments.

JA0008315

(59) Cheng, C. P.; Brown, T. L. *J. Am. Chem. Soc*. **1979**, *101*, 2327.